SUPPLEMENTARY INFORMATION

High-performance anode material for Li-ion batteries from bismuth molybdate incorporating F-free binder

To Giang Tran[a,b], Thuy-An Nguyen[c,d], Viet Duc Phung[c,d], Dinh Quan Nguyen[e,f], Thanh Ngoc Nguyen[g,h], Dang Manh Le[g,h], Hieu Trung Bui[g,h***], Il Tae Kim[i**], Tran Thi Kieu Ngan[i], Tuan Loi Nguyen[c,d*]

[a.] *Institute of Research and Development, Duy Tan University, Da Nang, Vietnam*
[b.] *School of Engineering & Technology, Duy Tan University, Da Nang, Vietnam*
[c.] *Institute of Fundamental and Applied Sciences, Duy Tan University, Ho Chi Minh City 70000, Vietnam*
[d.] *Faculty of Environmental and Chemical Engineering, Duy Tan University, Da Nang City 50000, Vietnam*
[e.] *Laboratory of Biofuel and Biomass Research, Faculty of Chemical Engineering, Ho Chi Minh City University of Technology (HCMUT), 268 Ly Thuong Kiet Street, Dien Hong Ward, Ho Chi Minh City, Vietnam*
[f.] *Vietnam National University Ho Chi Minh City, Linh Xuan Ward, Ho Chi Minh City, Vietnam*
[g.] *NTT Hi-Tech Institute, Nguyen Tat Thanh University, Ho Chi Minh City, Vietnam*
[h.] *Nguyen Tat Thanh University Center for Hi-Tech Development, Saigon Hi-Tech Park, Ho Chi Minh City, Vietnam*
[i.] *School of Chemical, Biological & Battery Engineering, Gachon University, Seongnam-si, Gyeonggi-do, 13120, Republic of Korea*

* Corresponding authors

To determine the content of crystalline and amorphous phases in the BMO sample, the areas of the diffraction peaks and the total area of the XRD spectrum were calculated using OriginPro software. The ratio between the two phases was calculated using **Eqs. S1** and **S2**.

$$\%\ Crystalline = \frac{S_P}{S_T} \qquad (S1)$$

$$\%\ Amorphous = \frac{(S_T - S_P)}{S_T} \qquad (S2)$$

Here, S_P represents the total integrated area of the diffraction peaks, while S_T denotes the overall area of the diffraction pattern, including contributions from both crystalline and amorphous phases.

Table S1. EDS result of the BMO material

	Bi	**Mo**	**O**
Weight (%)	65.37	19.82	14.81
Atom (%)	21.64	14.29	64.06

Table S2: Comparative evaluation of bismuth-based anode materials for LIBs.

Bismuth-based anodes	Current density ($mA\ g^{-1}$)	Cycle/Capacity ($mAh\ g^{-1}$)	Reference
Bi_2O_3@Bi_2MoO_6_400℃	0.1	80/701	[1]
$Bi_4Ge_3O_{12}$ NSs@NF	0.1	88/709	[2]
Bi_2MoO_6@C	0.1	300/618	[3]
Core-shell Bi@C	0.1	100/518	[4]
Bi_2S_3/C	0.12	50/472	[5]
Bi_2S_3/rGO	0.1	50/401	[6]
BMO_PAA	0.1	60/738	This work

Table S3. The resistances of BMO electrodes.

	R_s (Ω)	R_{SEI} (Ω)	R_{CT} (Ω)
BMO_PVDF	3.92 (± 0.04)	11.95 (± 0.46)	56.19 (± 0.79)
BMO_PAA	2.55 (± 0.03)	1.16 (± 0.06)	5.19 (± 0.25)

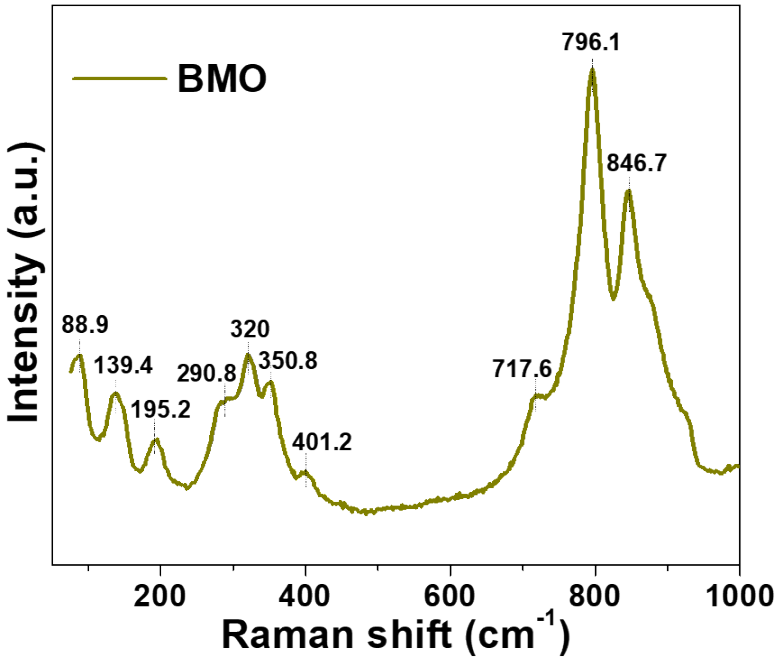

Fig. S1. Raman spectrum of the BMO material.

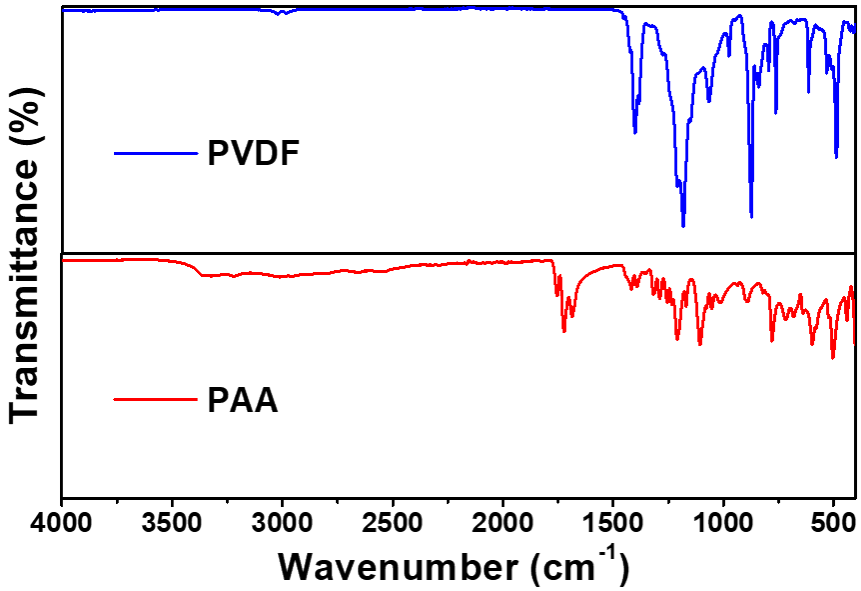

Fig. S2. FTIR results of PVDF and PAA binders.

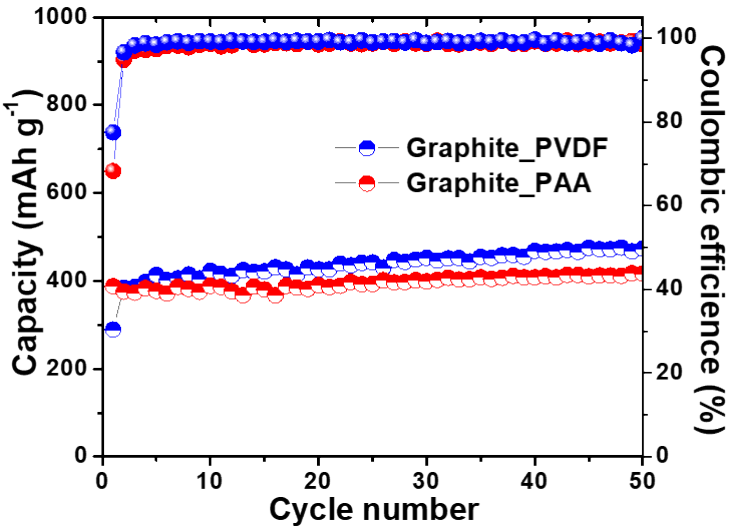

Fig. S3. Cycling performance of two electrodes: Graphite_PAA and Graphite_PVDF.

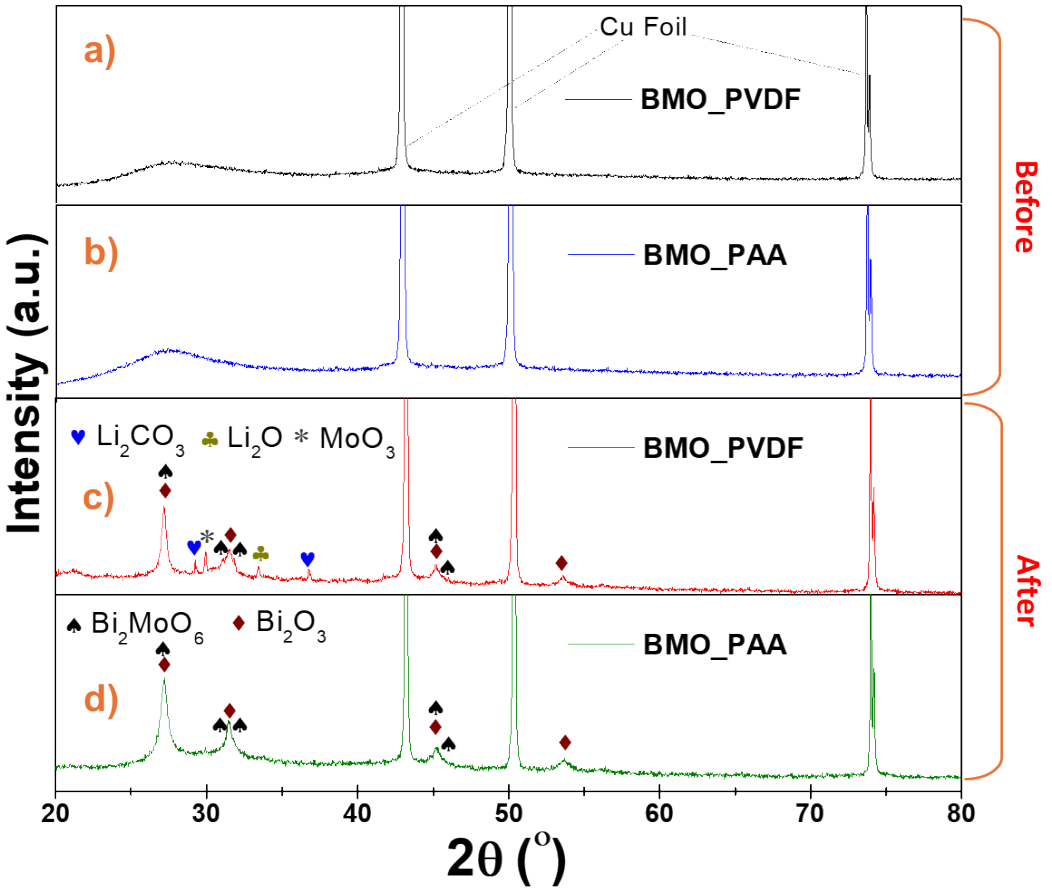

Fig. S4. XRD patterns of BMO_PVDF and BMO_PAA electrodes before (a, b) and after (c, d) cycling.

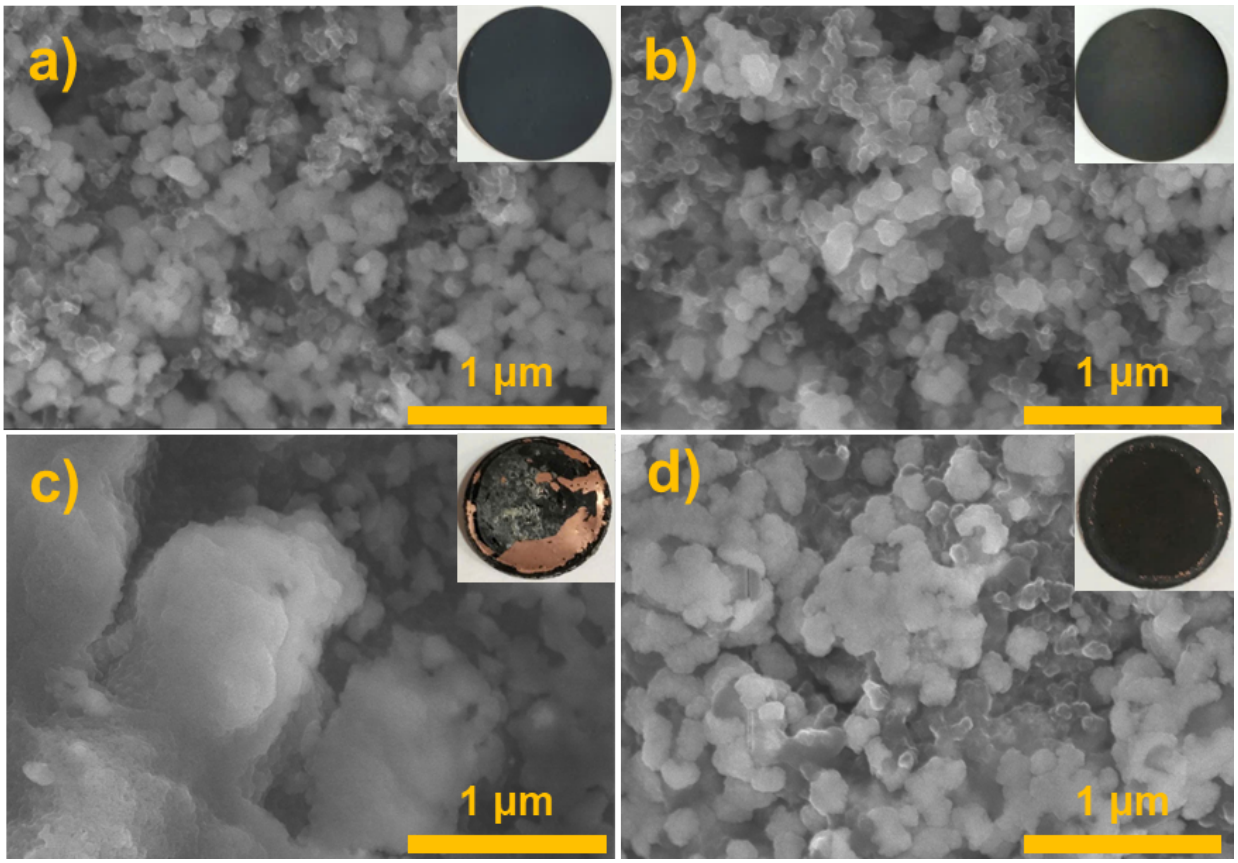

Fig. S5. SEM images and electrode photographs (insets) of BMO_PVDF and BMO_PAA electrodes before (a, b) and after (c, d) cycling.

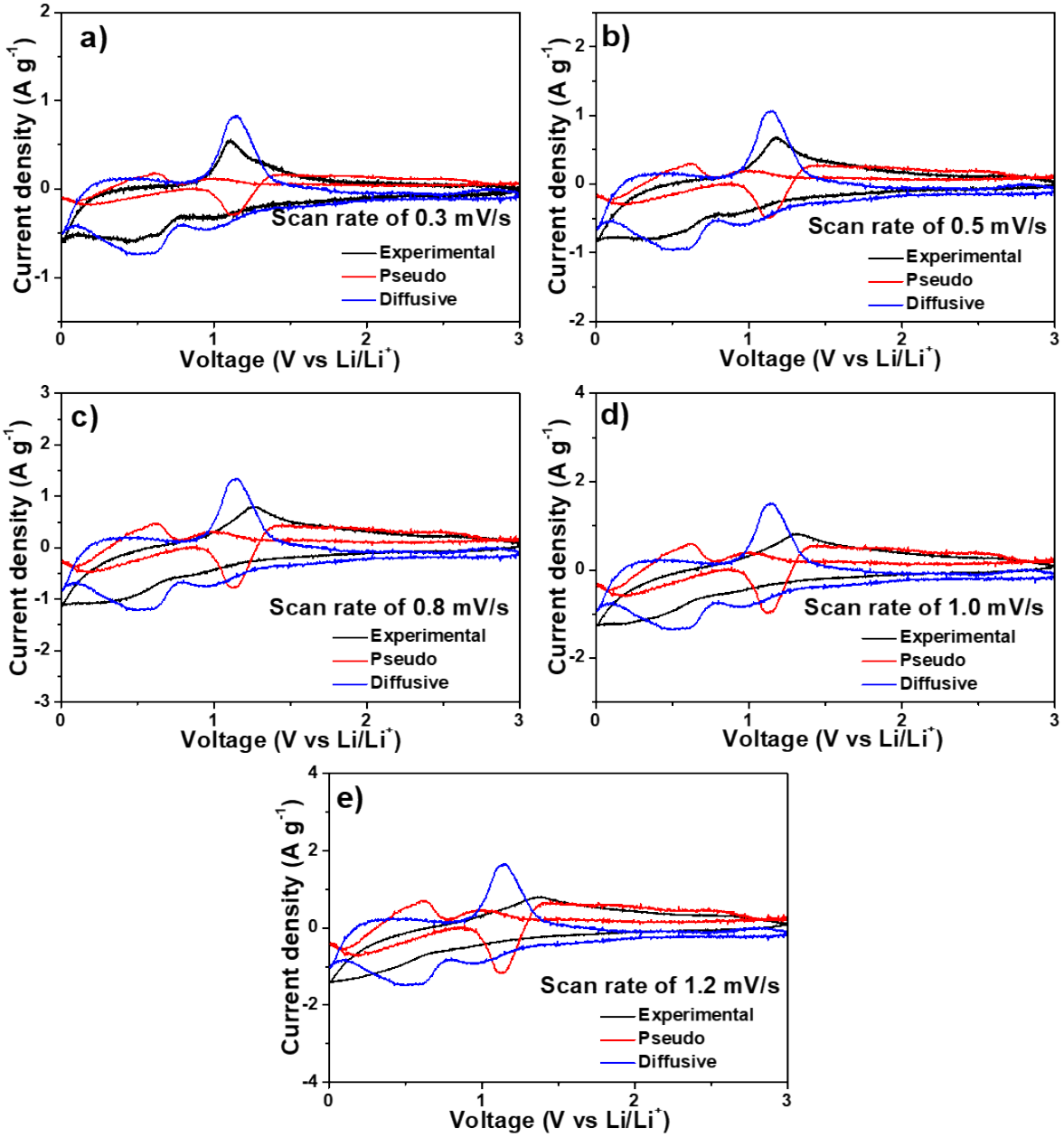

Fig. S6. (a–e) Pseudo and diffusive curves of BMO_PVDF electrode at five scan rates ranging from 0.3 to 1.2 mV s^{-1}.

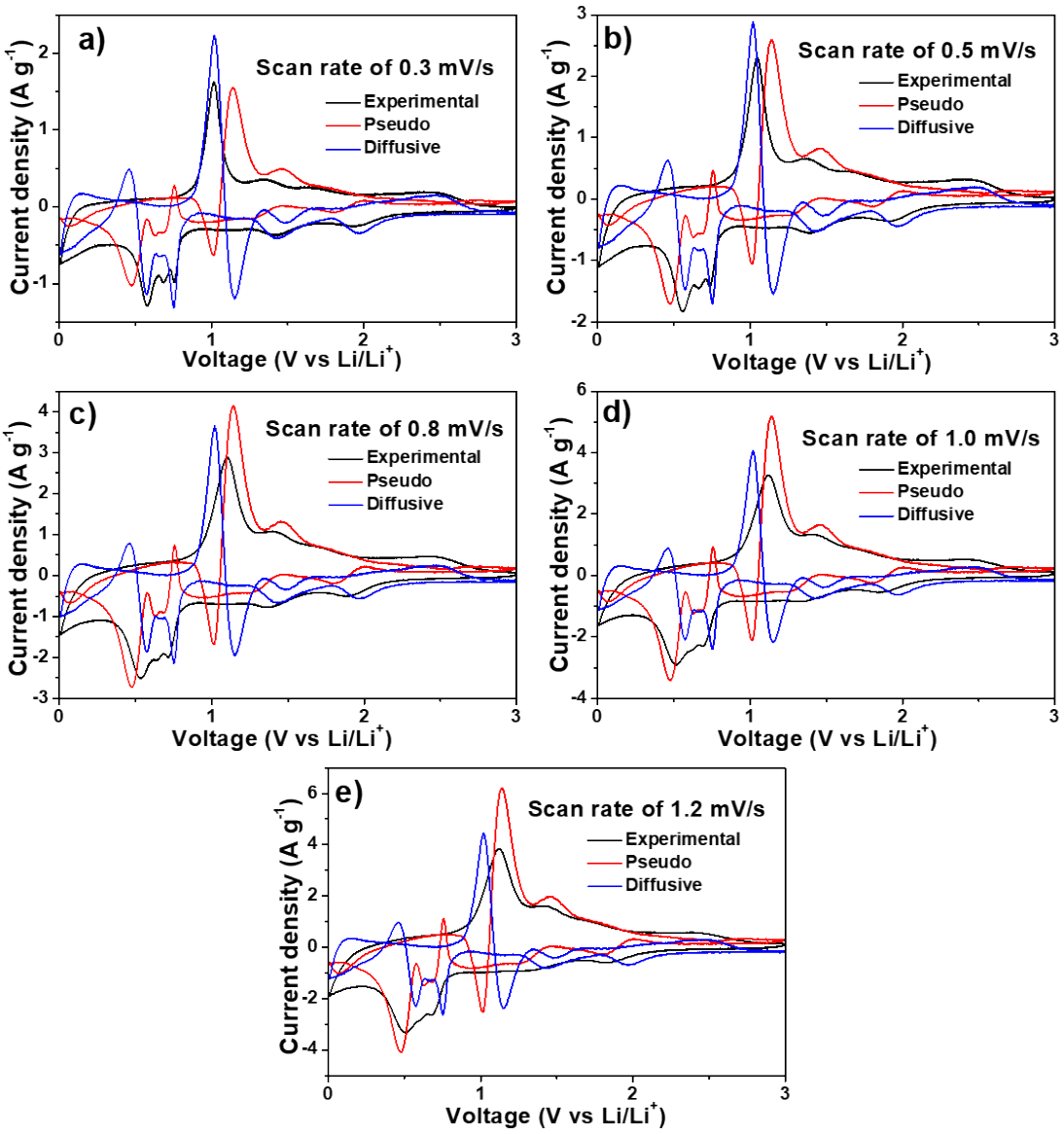

Fig. S7. (a–e) Pseudo and diffusive curves of BMO_PAA electrode at five scan rates ranging from 0.3 to 1.2 mV s^{-1}.

References

1 T. G. Tran, T. N. Nguyen, N. P. T. Le, L. T. Pham, M. V. Tran, Q. Q. Viet Thieu, T. L. Nguyen and D. Q. Nguyen, *Ceram. Int.*, 2024, **50**, 43710–43718.

2 J. Xu, W. Wei, X. Zhang, L. Liang and M. Xu, *Chin. Chem. Lett.*, 2019, **30**, 1341–1345.

3 X. Deng, X. Zhao, X. Zhang, L. Zhang and J. Zhang, *Inorg. Chem. Commun.*, 2025, 115439.

4 H. Fu, C. Shi, J. Nie, J. Wang and S. Yao, *J. Alloys Compd.*, 2022, **918**, 165666.

5 Y. Zhao, D. Gao, J. Ni, L. Gao, J. Yang and Y. Li, *Nano Res.*, 2014, **7**, 765–773.

6 Z. Zhang, C. Zhou, L. Huang, X. Wang, Y. Qu, Y. Lai and J. Li, *Electrochim. Acta*, 2013, **114**, 88–94.